JOURNAL OF PROPULSION AND POWER
Vol. 10, No. 4, July–Aug. 1994

Experimental Study of a Model Gas Turbine Combustor Swirl Cup, Part II: Droplet Dynamics

Hongyu Wang,* Vincent G. McDonell,† William A. Sowa,‡ and Scott Samuelsen§
University of California, Irvine, Irvine, California 92717

As the second part of a study to characterize the performance of a 3x scale gas turbine combustor swirl cup, the focus of the present article addresses the droplet dynamics. Droplet axial, radial, and tangential velocities as well as size were measured using phase Doppler interferometry. Bimodal droplet axial and tangential velocities distributions were observed in the shear layer close to the exit plane of the swirl cup. Bimodal droplet radial velocity distributions around the closing point of the on-axis recirculation zone and at the periphery of the spray were observed as well. Droplet velocity histograms, based on droplet size classes, reveal how these velocity bimodal distributions are formed and explain why velocity fluctuations for larger droplets are greater than those of the smaller droplets in some regions. Correlations between size and velocity, individual velocity components, and size and flow angle provide evidence of intermittent flowfield structures superimposed on the local and global turbulence. Specific flowfield structures and flowfield intermittancies are found to give rise to these bimodal distributions. Overall, these data add measurably to the understanding of the two-phase transport that can occur in practical systems.

I. Introduction

IN the first part of this study,[1] the *time-averaged* structure of the two-phase flowfield downstream of a coaxial counterswirling dome swirl cup is presented. This part of the study examines the *transient structure* of the droplets. In each case, a 3x scale model of a GE CFM 56 engine combustor dome swirl cup is used.[1]

The objectives of this article are 1) to provide insight into the mechanisms that give rise to the bimodal droplet velocity distributions that are produced by the swirl cup, and 2) to present a picture of the manner by which the droplets of different size are transported in the swirl cup flowfield. A foundation is laid for a longer range effort to correlate local droplet behavior to the overall performance of the dome swirl cup combustor in areas such as combustion instability, flow- and combustion-induced noise, and pollutant emissions.

Details regarding the instrumentation and facility used are available in Ref. 1. To provide perspective necessary for the following discussion, it is noteworthy that the measurements were obtained using a two-component phase Doppler interferometer. In order to measure each of the three components of velocity, it was necessary to conduct measurements along two orthogonal radial traverses. As a result, the axial and radial velocities were simultaneously measured along the "Y" traverse, while the tangential velocities were measured, with a repeat of the axial velocities, along the "X" traverse. While both traverses correspond to a radial traverse in this "axisymmetric" flow, the fact that radial and tangential velocities were not measured simultaneously is important.

Received March 20, 1992; revision received Oct. 21, 1993; accepted for publication Nov. 21, 1993.

*Research Assistant, UCI Combustion Laboratory. Student Member AIAA.

†Senior Research Engineer, UCI Combustion Laboratory. Member AIAA.

‡Associate Director, UCI Combustion Laboratory.

§Professor, Director, UCI Combustion Laboratory. Associate Fellow AIAA.

II. Results and Discussion

A. Droplet Velocity Bimodal Distributions

When considering the single-phase flow, bimodal velocity distributions can be produced by large flowfield structures, form intermittancies, or both. These same influences can result in bimodal droplets velocity distributions in a two-phase flow as well. In addition, droplets issuing from the swirl cup are influenced by the gas phase as a function of droplet size (i.e., Stokes number), and can arrive at a given point from different sources (e.g., directly from the atomizer or from reatomization off the primary venturi of the swirl cup). Hence, the "history" of the individual droplets arriving at a given point in the flow results in a complex behavior that is not associated solely with that of the gas phase.

Bimodal droplet velocity distributions were documented at four locations in the spray, as shown in Fig. 1. A different mechanism was found to be responsible for the bimodal droplet velocity distributions at each point. In the discussion that follows, the mechanisms associated with the axial, tangential, and radial velocity bimodal distributions are described.

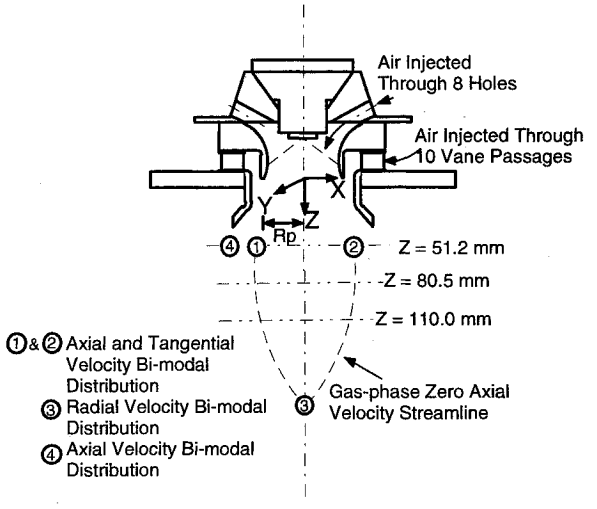

Fig. 1 Swirl cup assembly and four velocity bimodal distributions.

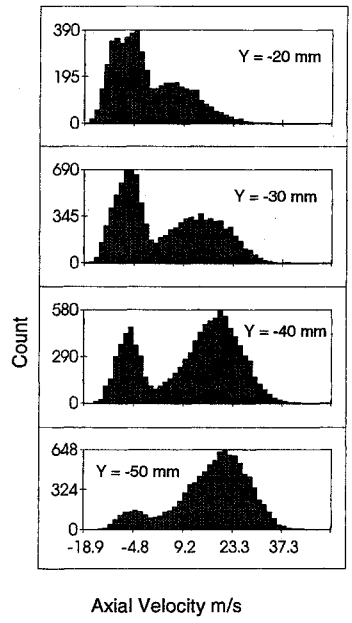

Fig. 2 Axial velocity histograms: $X = 0$ mm, $Z = 51.2$ mm.

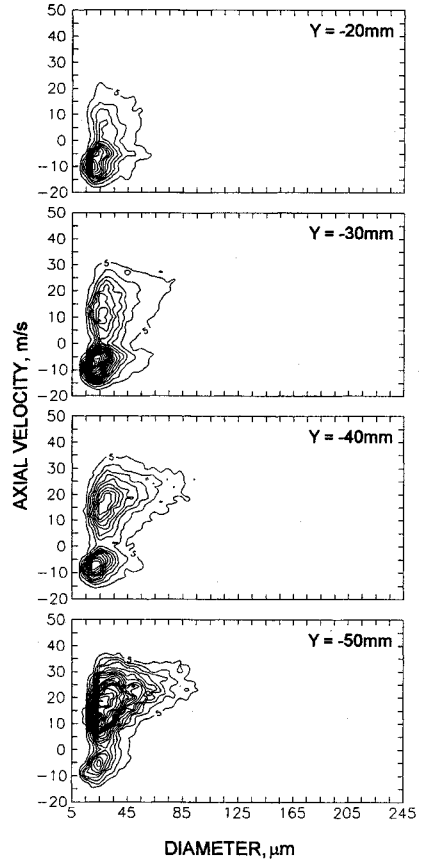

Fig. 3 Size-axial velocity correlation: $X = 0$ mm, $Z = 51.2$ mm.

1. Bimodal Axial Velocity

Bimodal droplet axial velocity distributions are observed at location ① along the Y traverse at $Z = 51.2$ mm. This region is the shear layer between the primary and secondary airstreams. Figure 2 presents droplet axial velocity distributions at four different locations along the Y axis. From the centerline outwards, the bimodal droplet axial velocity distributions shift from reverse-flow dominated to downstream-flow dominated. The bimodal droplet axial velocity distribution is observed only at the axial plane nearest the exit plane of the swirl cup. Further downstream, the bimodal

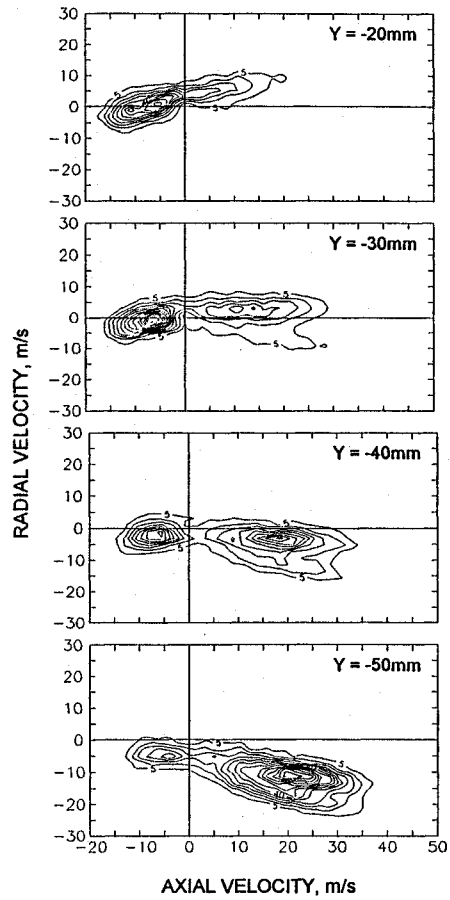

Fig. 4 Axial velocity-radial velocity correlation: $X = 0$ mm, $Z = 51.2$ mm.

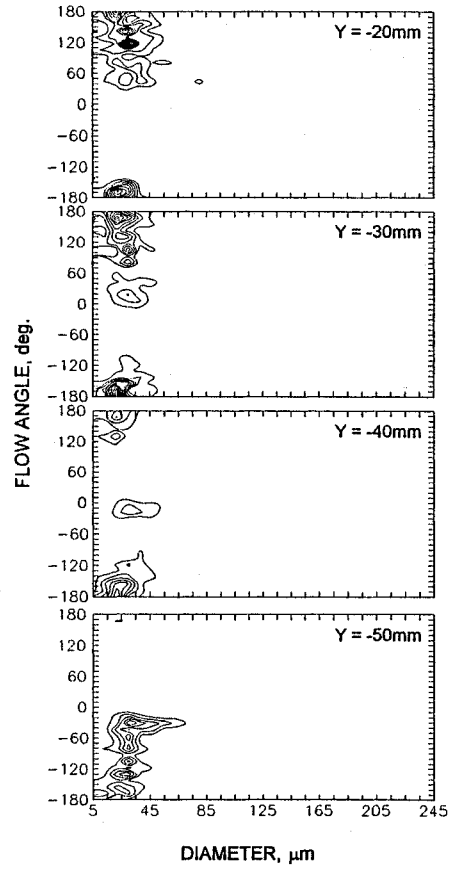

Fig. 5 Size-flow angle correlation: $X = 0$ mm, $Z = 51.2$ mm.

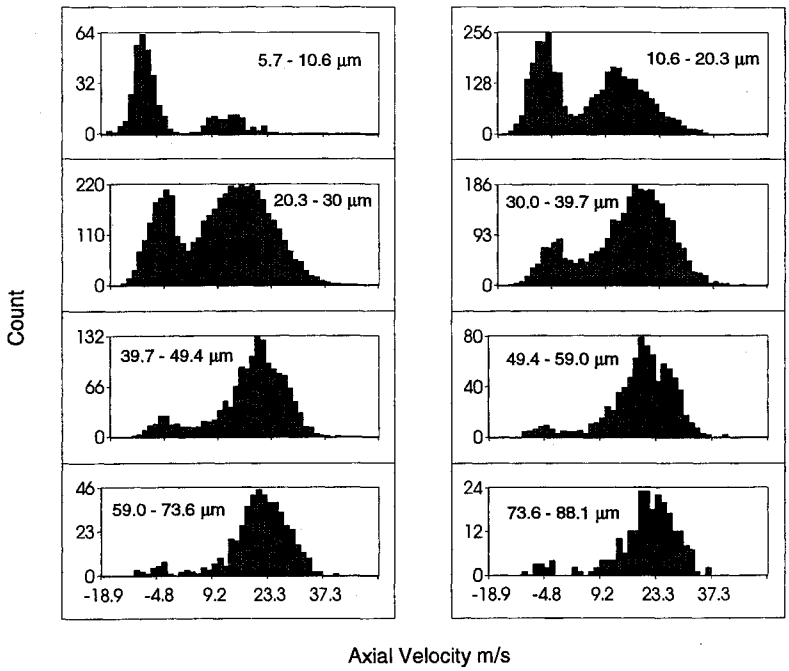

Fig. 6 Axial velocity histograms based on discrete droplet size classes: $X = 0$ mm, $Y = -40.0$ mm, $Z = 51.2$ mm.

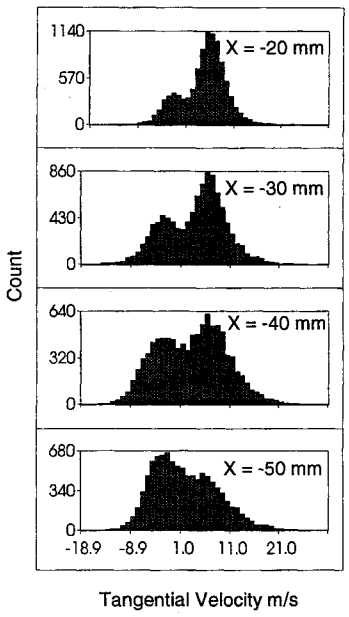

Fig. 7 Tangential velocity histograms: $Y = 0$ mm, $Z = 51.2$ mm.

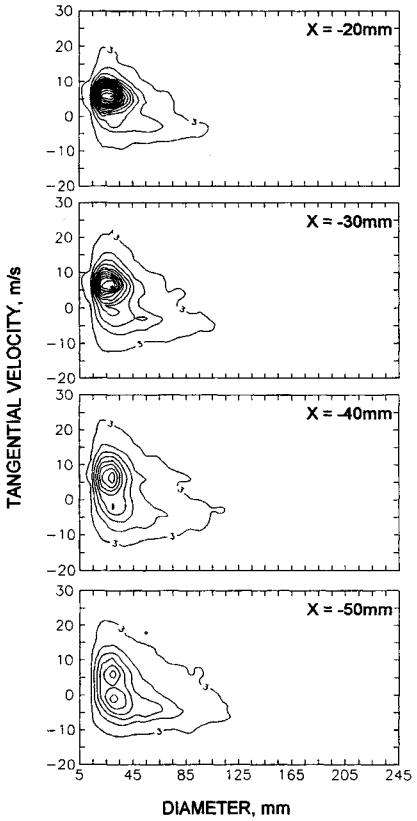

Fig. 8 Size-tangential velocity correlation: $Y = 0$ mm, $Z = 51.2$ mm.

structure vanishes due to 1) more uniform mixing of the droplets into the air stream, 2) a decrease in local droplet loading rate, and 3) a decay in droplet axial momentum.

Figure 3 shows the corresponding size-axial velocity correlations. Droplets smaller than 60 μm in diam travel upstream near the centerline and downstream at the locations away from the centerline. A systematic transition from the upstream to downstream flow occurs as the sampling location moves radially outwards. Note that more larger droplets at higher axial velocities are detected as the measurement moves radially outwards.

The axial velocity-radial velocity correlations are shown in Fig. 4. (In the coordinate system used in this study, negative velocities represent radial velocities away from the centerline for $-Y$ locations.) With increasing distance from centerline, the droplets primary direction transitions from upstream and away from centerline to downstream and towards the centerline. Note that, at $Y = -30$ and -40 mm, no dominant radial velocity occurs, yet the axial velocity distribution is bifurcated, with a distinct group moving upstream and another downstream.

The size-flow angle correlations in the R-Z plane are shown in Fig. 5 at different distances from centerline. Following the convention adopted in the operating manual (Aerometrics PDPA 3100-S), a flow angle of 0 deg corresponds to flow in the downstream direction, and flow angles of 180 and -180 deg represent flow upstream. A flow angle of 90 or -90 deg corresponds to flow in the radial direction towards and away from the centerline, respectively. Larger droplets (greater

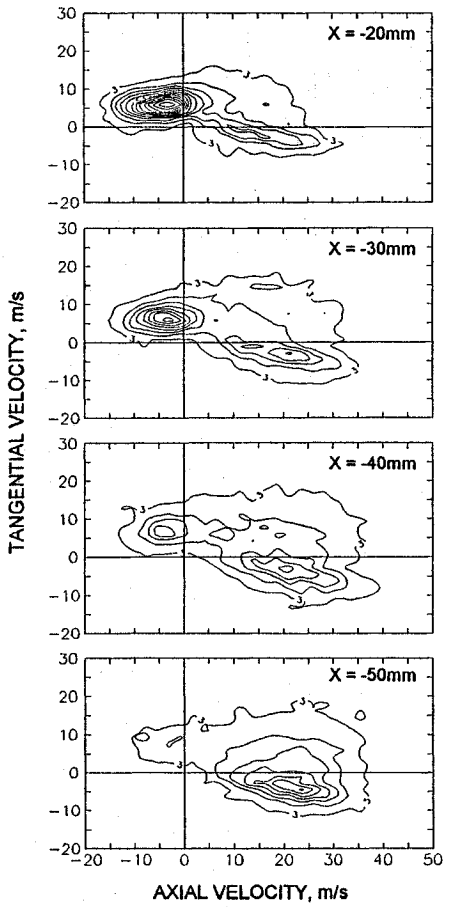

Fig. 9 Axial velocity-tangential velocity correlation: $Y = 0$ mm, $Z = 51.2$ mm.

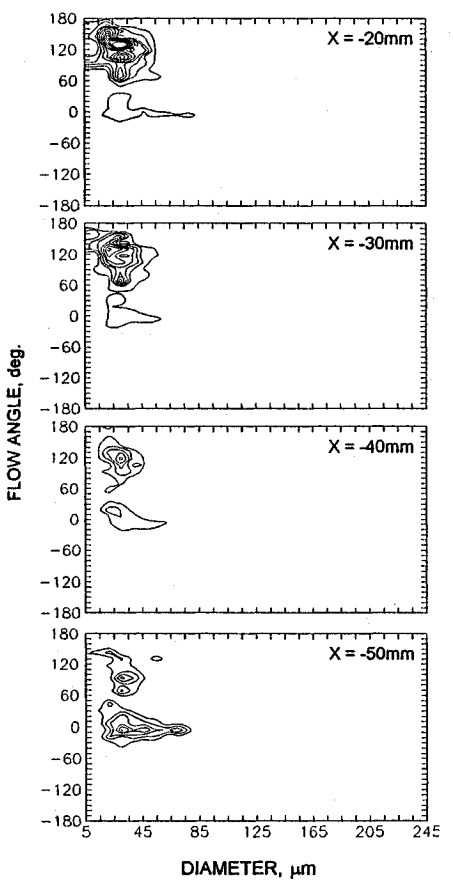

Fig. 10 Size-flow angle correlation: $Y = 0$ mm, $Z = 51.2$ mm.

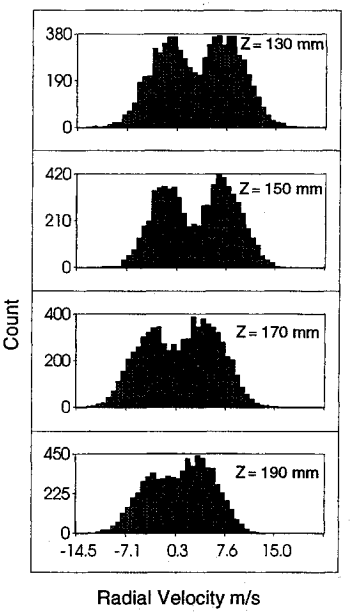

Fig. 11 Radial velocity histograms: $X = 0$ mm, $Y = 0$ mm.

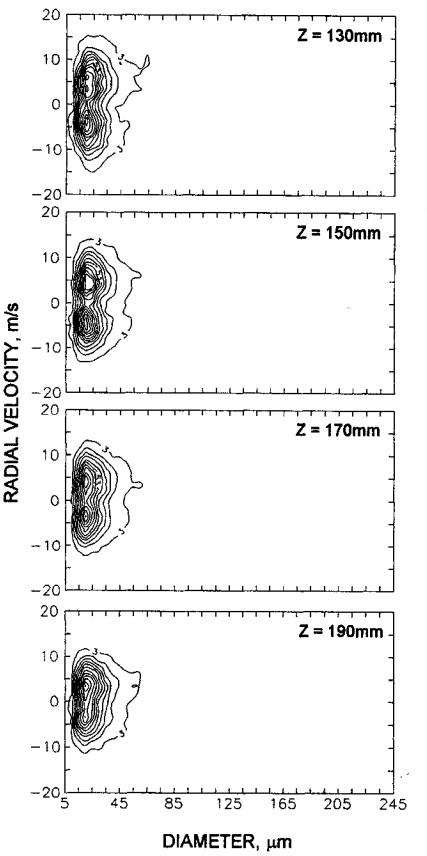

Fig. 12 Size-radial velocity correlation: $X = 0$ mm, $Y = 0$ mm.

than 85 μm in diam) move within a narrow range of angles away from the centerline regardless of radial location. As observed previously, the number of larger droplets detected increases with increasing distance away from centerline.[1] In the recirculation zone, the smaller droplets flow in two distinct directions, straight upstream, or away from the centerline with a sharp angle. These directions correspond to the following sources of droplets: 1) those recirculated from downstream (moving straight upstream), 2) those issuing directly from the atomizer and not impacting the primary venturi (moving away from the centerline and downstream), and 3) the primary venturi (those moving mainly towards the centerline and downstream).

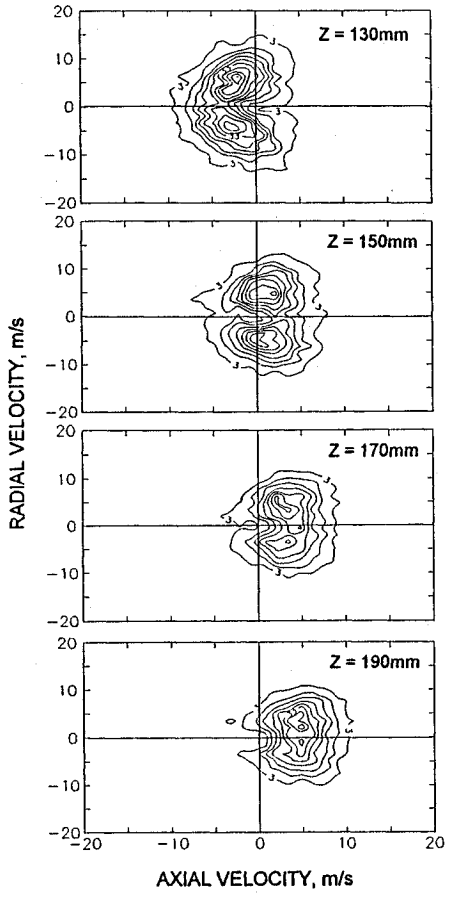

Fig. 13 Axial velocity-radial velocity correlation: $X = 0$ mm, $Y = 0$ mm.

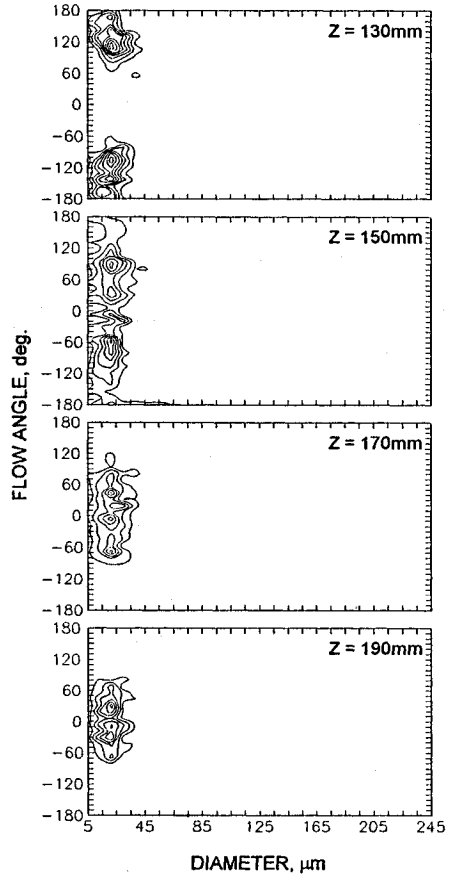

Fig. 14 Size-flow angle correlation: $X = 0$ mm, $Y = 0$ mm.

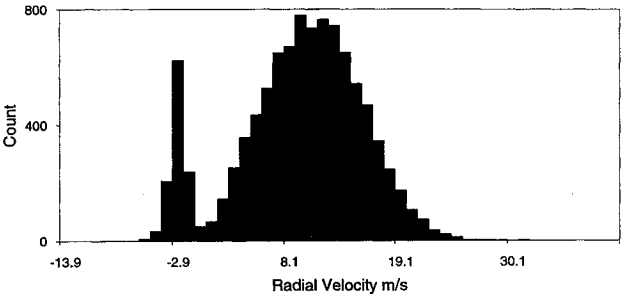

Fig. 15 Radial velocity histogram: $X = 0$ mm, $Y = 80$ mm, $Z = 51.2$ mm.

Further analysis of the nature of the axial velocity bimodal distribution was conducted by constructing velocity histograms based on the discrete droplet size classes. As an example, Fig. 6 shows the axial velocity histograms based on droplet size subranges in the shear layer close to the exit plane of the swirl cup at the position $X = 0.0$, $Y = -40.0$ mm, and $Z = 51.2$ mm. It can be seen that the smaller droplets (5.7–20 μm) contribute mainly to the peak in the negative axial velocity; the droplets with moderate size (20–30 μm) contribute equally to both peaks in the histogram; most of the larger droplets greater than 30 μm contribute mainly to the positive velocity. The apparent paradox that droplets of the same size can travel in opposite directions is a direct result of the different sources of droplets in the swirl cup — those from the atomizer proceed downstream, whereas those produced by the primary venturi travel downstream and are then recirculated back toward the swirl cup. The range of axial velocities for both larger and smaller droplets is similar in the region close to the centerline, but the velocity distribution for larger droplets is flatter and wider than that for smaller droplets, resulting in a larger standard deviation (i.e., rms velocity). This provides one reason why the axial fluctuating velocity of larger droplets is greater than that of smaller droplets in the region close to centerline.[1]

Droplets of different size play a different role in forming the axial velocity bimodal distribution. For example, more smaller droplets join the upward recirculating flow than do larger droplets. The point in space where a droplet joins the recirculating flow (i.e., the depth of droplet penetration into the recirculation zone), depends upon its size (i.e., inertia) and from where it traveled to arrive at the point (i.e., history). Since moderate-sized drops move both upstream and downstream at this point, the apparent "fluctuating" velocity of these droplets is greater than that for any other droplet size class. In summary 1) velocity histograms based on droplet size classes are an effective tool in providing insight into droplet motion, and 2) the droplet fluctuating velocity should not be interpreted in the same manner as a local variation in the gas-phase velocity.

2. *Bimodal Tangential Velocity*

Bimodal droplet tangential velocity distributions were observed at location ② along the X traverse (Fig. 1) which corresponds to a similar radial location in the flow as location ①, but 90-deg rotated with respect to the centerline. These distributions are presented in Fig. 7 as a function of distance from centerline. Positive velocities on the $-X$ side represent rotation in the counterclockwise direction (corresponding to the rotating direction of the secondary airflow) looking downstream from the top of the swirl cup. The counterclockwise swirl becomes weaker and the clockwise swirl becomes stronger with increased distance from the centerline, indicating that the flow is more affected by the primary clockwise swirling airstream at locations away from the centerline.

Figure 8 shows the correlations between droplet size and the tangential velocity. The larger droplets display a greater tendency to flow in a clockwise motion while the smaller droplets move counterclockwise in the recirculation zone. This

is attributed to 1) the ability of the larger droplets injected directly from the atomizer to retain the influence of the primary airstream, and 2) the tendency of the smaller droplets to follow the continuous-phase streamlines irrespective of their point of origin.

Figure 9 presents correlations between the axial and tangential velocities. Three distinct types of droplet groupings are observed. The first occurs at $X = -20$ mm where a significant number of droplets move counterclockwise and upstream. The velocities associated with this group are correlated with the recirculating flow. As the measurement location progresses radially outwards, the grouping transitions to a second type, droplets moving clockwise and downstream. This group of droplets come from the atomizer directly and retain the influence of the primary swirling air. The last type of droplet grouping reflects droplets moving downstream while rotating counterclockwise. These droplets come from the edge of the primary venturi. This correlation again confirms the existence of three sources of droplets.[1]

Figure 10 shows the size-flow angle correlation in the Θ-Z plane, where Θ is the tangential direction. The smaller droplets flow in many different directions while the larger droplets move almost entirely in one direction. These results suggest that 1) the mechanism for the mixing for the smaller droplets is more chaotic and dependent upon the local flow dynamics, and 2) mixing of larger droplets is difficult to achieve due to the large momentum of these drops.

3. *Bimodal Radial Velocity*

Bimodal droplet radial velocity distributions were observed at location ③ at the centerline, corresponding to the point of closure of the on-axis recirculation zone, and at location ④ (the spray periphery). The former is due to the instability of the flow around the stagnation point (e.g., precession), as shown in Fig. 11, whereas the latter is due to the air entrainment at the spray periphery where fine particles are essentially stopped by the relatively quiescent environment and drift about with very small velocities.

In Fig. 12, the size-radial velocity correlations along the centerline reveal two clusters of radial velocities symmetric about the zero radial velocity. This figure also suggests that the mean radial velocity of droplets is independent of size, which was previously observed.[1] This may explain why the fluctuating radial velocity reaches a maximum around the stagnation point along the centerline.[1]

The axial-radial velocity correlations are shown in Fig. 13. Moving downstream, a collapse in the range of radial velocities is evident. Note that, upstream of the closure point of the recirculation zone, most of the droplets that have a radial velocity close to zero have a negative axial velocity (indicating entrainment into the recirculation zone). This trend reverses downstream of the closure point, where most of the droplets with near zero radial velocities have a positive axial velocity (moving downstream out of the recirculation zone). Fewer droplets possess near zero axial and radial velocity at the same time.

The size-flow angle correlations are shown in Fig. 14. Two groupings of flow angles symmetric about the centerline are evident. These two different flow angles likely correspond with a form intermittency of the flowfield associated with the contraction of the recirculation zone around the stagnation point.

A bimodal droplet radial velocity distribution was also observed at the periphery of the spray (location ④: $X = 0$ mm, $Y = 80$ mm, and $Z = 51.2$ mm) due to the entrainment of air containing slow-moving smaller droplets which appear as a local peak near 0.0 m/s as shown in Fig. 15.

Further insight into this structure is provided by Fig. 16, which shows the radial velocity histograms for different size subranges at the spray periphery. Small droplets (10–30 μm) contribute to both peaks in the histograms. This suggests that droplets with different points of origin are mixing at this sample location. The entrained droplets come from the recirculating mist around the periphery of the spray.

In summary, bimodal axial velocity distributions arise due to the different inertia and initial momentum of droplets of different size. The smaller droplets tend to follow the recirculating flow more easily than the larger droplets. This mechanism is also partly associated with the bimodal tangential velocity distribution. Another factor in the formation of tangential velocity bimodal distributions is the different sources of droplets. Two types of bimodal radial velocity distributions were observed. One is associated with the contraction around the closure point of the recirculation zone and is likely a result to a form intermittency. The second is associated with the air entrainment at the spray periphery.

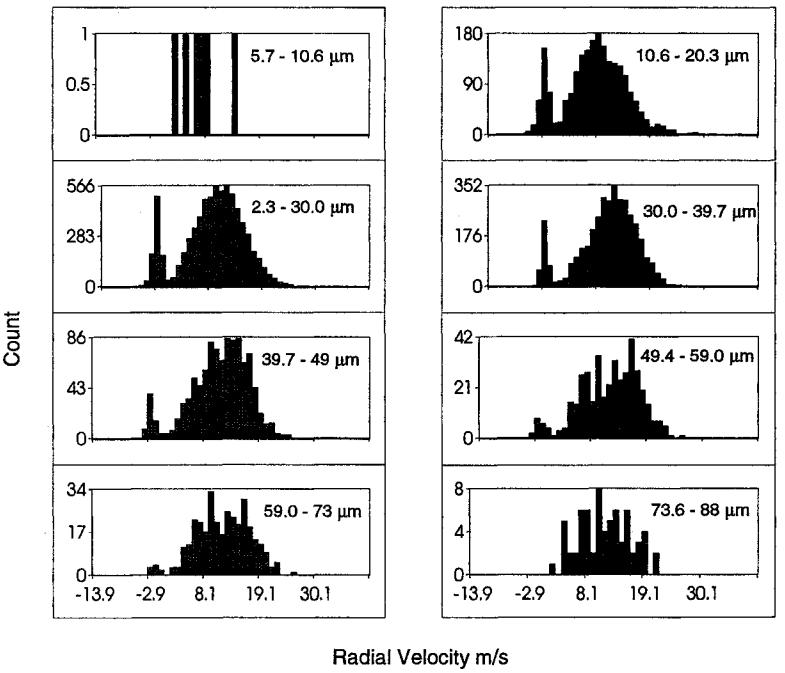

Fig. 16 Radial velocity histograms based on discrete droplet size classes: $X = 0$ mm, $Y = 80$ mm, $Z = 51.2$ mm.

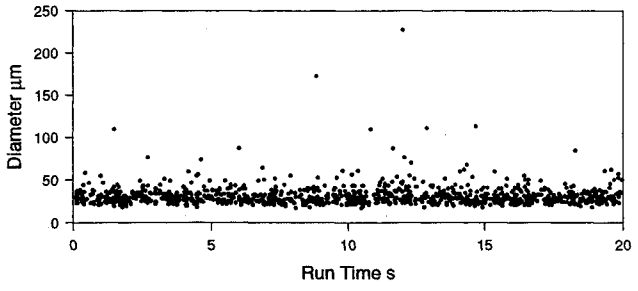

Fig. 17 Droplet arrival within t = 0.0–2.5 s: X = 0 mm, Y = −40 mm, Z = 51.2 mm.

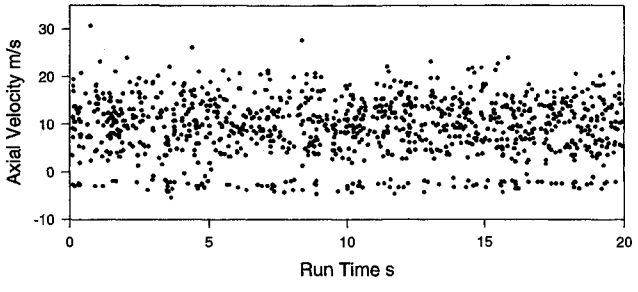

Fig. 18 Time sequence of axial velocity t = 0.0–2.5 s: X = 0 mm, Y = −40 mm, Z = 51.2 mm.

B. Temporal Measurement Results

In order to further understand the nature of the bimodal axial velocity distributions, time-of-arrival data were acquired and analyzed to characterize the temporal behavior of droplets. Figure 17 shows the arrival of droplets over a 0.25-s sampling period in the shear layer at the position X = 0.0, Y = −40.0 mm and Z = 51.2 mm. Although some distinct groups of drops (i.e., "clusters") appear, the grouping in the present case is less pronounced compared to a simplex atomizer spray in the absence of swirling airstreams.[2] This suggests that the complex aerodynamic flowfield of the swirl cup produces a random droplet arrival that is not correlated with time or droplet size. However, these results do not address whether a particular size occurs regularly.

Figure 18 presents the correlation between the droplet velocities and time. Unlike the size-time results, two distinct velocities tend to be measured with high probability. This cannot be explained by considering the local turbulence fluctuations since the fluctuations are not of the same order of the local continuous phase turbulent fluctuations. These results are further evidence of the large-scale structure influence and the ballistic behavior of droplets from different origins.

III. Conclusions

Spatially and temporally resolved data have been used to analyze the droplet dynamics produced by a model combustor swirl cup featuring two coaxial, counterswirling airstreams. The significant conclusions that resulted from the study are as follows:

1) The aerodynamic flowfield influences the motion of droplets as a function of size and, as a result, influences how each drop size contributes to forming bimodal velocity distributions.

2) Bimodal axial, radial, and tangential velocities distributions were observed. The mechanism responsible for the bimodal distribution depends on the location in the flow. In general, the bimodal distributions are correlated with large structures in the aerodynamic flowfield such as the recirculation zone, the shear layer of the counter-rotating airstreams, the closure point of the recirculation zone, and the air entrainment at the spray periphery. For example, the bimodal radial velocity distribution around the closing point of the recirculation zone is likely associated with form intermittency. As further evidence of large structures, time sequences reveal the presence of two dominant velocities.

3) The magnitude of the droplet fluctuating velocity is correlated with not only the gas-phase local velocity fluctuation but also the droplet-time history and trajectory. Hence, droplet ballistic behavior and size-velocity correlation must be considered when interpreting droplet fluctuating velocity. This explains why, in some cases, the larger droplets show a greater fluctuation in axial velocity than do the smaller droplets.

4) Tools (such as droplet velocity histograms based on discrete droplet size classes, temporal-resolved measurement, and size-velocity, individual velocity components, and size-flow angle correlations) used in the present study to identify the mechanisms forming droplet velocity bimodal distributions can be effectively employed to analyze droplet behavior in other complicated flow configurations. For example, droplet velocity histograms for discrete size classes can provide more accurate initial and boundary conditions for the numerical modeling than droplet mean and fluctuating velocities alone, and facilitate as well the examination of the modeling results in a more critical way.

Although this study utilized a model of production gas turbine hardware, the extent to which these results may be directly applied to actual operating conditions (high-pressure, high preheat temperature, reacting) has yet to be addressed. This notwithstanding, the data reveal the inherent complexities that must be considered in such applications and provide a data base for comprehensive codes, the latter of which can be used to then model practical conditions.

Acknowledgments

The authors acknowledge the financial support from GE Aircraft Engines and valued discussions with David Burrus, and the assistance from C. T. Brown and H. D. Crum during the tests.

References

[1]Wang, H. Y., Sowa, W. A., McDonell, V. G., and Samuelsen, G. S., "Experimental Study of a Gas Turbine Co-Axial Counter-Swirling Two-Phase Flow, Part I: Characterization of a Two-Phase Flowfield," *Journal of Propulsion and Power*, Vol. 10, No. 4, 1994, pp. 441–445.

[2]McDonell, V. G., "Evolution of Droplet/Gas Phase Interaction in Polydispersed Reacting and Non-Reacting Sprays," UCI Combustion Lab. Rept. ARTR-90-7, Univ. of California, Irvine, CA, 1990.